

Distortion effects in  $(\pi, \pi p)$  quasifree knockout reactions

L. Rees, N. S. Chant, and P. G. Roos

*Department of Physics and Astronomy, University of Maryland, College Park, Maryland 20742*

(Received 2 March 1982)

Distorted wave impulse approximation calculations for the  $(\pi, \pi p)$  quasifree knockout reaction on  $^{16}\text{O}$  and  $^{40}\text{Ca}$  have been carried out for a variety of bombarding energies and angle pairs. In general, the distortion effects arising from the interaction of the pions and protons with the target core are strong and vary with bombarding energy. The results emphasize the need to include these interactions properly in any analysis of experimental data.

$$\left[ \begin{array}{l} \text{NUCLEAR REACTIONS DWIA reaction theory of proton knockout} \\ \text{from nuclei } ^{16}\text{O}, ^{40}\text{Ca}(\pi^{\pm}, \pi^{\pm}p), T_{\pi}=100-300 \text{ MeV, calculate} \\ \sigma(\theta_1, \theta_2, E_1). \end{array} \right]$$

## I. INTRODUCTION

The availability of relatively high intensity, high quality pi-meson beams has led to a recent interest in the  $(\pi, \pi N)$  nucleon knockout reaction. There have been a series of abstracts<sup>1-5</sup> as well as several published papers<sup>6-8</sup> on experimental results for  $(\pi^{\pm}, \pi^{\pm}p)$  and  $(\pi^{\pm}, \pi^{\pm}n)$  reactions, generally with light target nuclei.

The interpretation of these measurements rests largely upon the applicability of a quasifree knockout description of the reaction mechanism. If this is indeed valid, the utility of such studies is twofold. Firstly, as is the case in other kinematically complete nucleon knockout experiments, such as  $(p, 2p)$  or  $(e, ep)$ , the  $(\pi, \pi N)$  reaction contains, in principle, detailed nuclear structure information on the single particle orbitals of nuclei. The availability of this information, however, depends greatly on the severity of distortion effects arising from projectile-core and ejectile-core interactions. For example, distorted wave impulse approximation (DWIA) calculations<sup>9</sup> of  $(p, 2p)$  show that much of the momentum space wave function information contained, in principle, in such reactions is obscured due to strong distortion effects. Similar DWIA calculations<sup>10</sup> show significant improvement for  $(e, ep)$  reactions, and aside from experimental difficulties, these reactions should provide more detailed nuclear structure information. Since the pi-meson is a strongly interacting particle, one might expect relatively large distortion effects similar to  $(p, 2p)$ . Thus, it is important to examine the distortion effects in comparison with other nucleon knockout

reactions in order to understand whether pion induced knockout reactions can make unique contributions to the study of nuclear structure.

The second, and perhaps more novel, aspect of  $(\pi, \pi N)$  reactions is the possibility of extracting information on the off energy shell behavior of the  $\pi$ - $N$  interaction. In the factorized DWIA the  $\pi$ - $N$  half off-shell cross section enters as a multiplicative factor, suggesting that  $(\pi, \pi N)$  results could be used to determine this quantity rather directly. Since little is known of the off-shell  $\pi$ - $N$  behavior, and since these matrix elements (either half or fully off-shell) enter into essentially all  $\pi$ -nucleus reactions, the possibility of extracting such information from measurements of the  $(\pi, \pi N)$  reaction is attractive.

Similar hopes have long been held for  $(p, 2p)$  reactions. However, particularly for cases which can be measured relatively easily, the extracted cross sections are rarely sufficiently far off shell to distinguish between different nucleon-nucleon potentials. Experimental geometries which, in principle, determine nucleon-nucleon matrix elements further off-shell generally have several problems: (a) they sample momentum regions where the bound nucleon momentum wave function is small and therefore poorly known; (b) distortion effects arising from interactions with the core are very large; and (c) the factorization approximation utilized in most DWIA calculations may be poor.<sup>11</sup> For example, the  $N$ - $N$  matrix element is relatively far off shell in  $(p, 2p)$  geometries in which two protons exit at small angles with comparable energies. In this case the major difficulties are (b) and (c). As a result of these various difficulties, essentially no reliable informa-

tion on the off-shell  $p$ - $p$  interaction has been extracted from  $(p, 2p)$  data so far.

Clearly, similar difficulties may impede  $(\pi, \pi N)$  studies. At a minimum one can expect that the extraction of  $\pi$ - $N$  off-shell information will necessitate an accurate treatment of distortion effects. This statement is true not only for geometries corresponding to points far off shell, but even for the more conventional cases where the bound nucleon wave function is relatively well known and one might expect the factorization approximation to be satisfactory. Even at these points the  $(\pi, \pi N)$  cross section may well be considerably reduced by distortion effects and the extraction of any half-shell cross sections could depend sensitively on their treatment.

The extraction of both nuclear structure and  $\pi$ - $N$  off-shell information is thus expected to depend heavily on the treatment of distortion effects. Examinations of the theoretical aspects of the  $(\pi, \pi N)$  reaction have been carried out by a number of authors. The simplest treatment of distortion effects due to the residual nucleus is the semiclassical model used by Sternheim and Silbar.<sup>12</sup> This model, which assumes classically attenuated straight line paths for the incident and emergent particles, allows for charge exchange by the outgoing nucleon. Although the model has been relatively successful in predicting inclusive yields such as those measured in radiochemical studies<sup>13</sup> or in nucleon singles spectra,<sup>14</sup> it is unlikely to provide a quantitative description of the detailed data obtained in high resolution exclusive  $(\pi, \pi N)$  measurements. This is particularly true at the lower pion energies where refraction and phase averaging inside the nucleus are likely to be important. Difficulties with this simple model are already observed in the prediction of the ratio of cross sections  $^{12}\text{C}(\pi^+, \pi^+ p)^{11}\text{B}$  to  $^{12}\text{C}(\pi^-, \pi^- p)^{11}\text{B}$  for low-lying states in  $^{11}\text{B}$ . Sternheim and Silbar<sup>12</sup> predict a ratio of 7.1 compared to the measured value<sup>7</sup> of  $14.0 \pm 2.6$ , the experimental value being in agreement with PWIA predictions.<sup>12</sup> This disagreement can result from the assumption of straight line trajectories or an overestimate of nucleon charge exchange, or both.

In their investigation of the  $(\pi, \pi N)$  reaction, Jackson, Ioannides, and Thomas<sup>15</sup> have basically restricted their attention to the study of off shell and nuclear medium effects on the  $\pi$ - $N$  vertex. Assuming a factorized form for the DWIA they have calculated the two-body  $\pi$ - $N$  half-off-shell cross section including Pauli blocking. The Pauli blocking is that appropriate for nuclear matter, and various densities (or equivalently Fermi momenta) are ex-

amined. The calculations of Ref. 15 imply that the differences between the half-off-shell and on-shell cross section are generally small, but that Pauli blocking effects may be large depending on the degree of radial localization. However, no distorted wave calculations were carried out to investigate their relative importance.

The most complete theoretical study to date of the  $(\pi, \pi N)$  reaction is that of Levin and Eisenberg.<sup>16</sup> They have carried out DWIA calculations for  $^{16}\text{O}(\pi^+, \pi^+ p)^{15}\text{N}$  at bombarding energies of 100, 130, and 165 MeV. These include both factorized DWIA calculations and nonfactorized calculations using a separable  $t$  matrix, as well as studies of specific off-shell behavior and the effect of a spin-orbit term in the exit nucleon potential. The calculations of Ref. 16 show the great importance of including distortion of the pion and proton wave functions which leads to approximately a factor of 5 reduction in the cross section at 130 MeV. Levin and Eisenberg also show that for their particular choice of the  $\pi$ - $N$  off-shell  $t$  matrix the factorization approximation is not an especially good approximation, particularly at the lowest energy. However, it should be noted that although the factorization approximation leads to changes in shape of the proton momentum distribution (such as at the ratio of the peaks for a  $p$ -state distribution), the magnitude of the cross section is nearly the same and these effects are generally small compared to the overall effect of including distortion. The authors also show that the shapes of the distributions are sensitive to other input such as the strength of the proton spin-orbit potential and the assumed off-shell behavior. Thus, detailed testing of the model and the goodness of the factorization approximation awaits more precise experimental data.

Because of the current experimental interest in  $(\pi, \pi N)$  reactions, and the eventual possibility of studying the off-shell behavior of the  $\pi$ - $N$  interaction, we have undertaken a series of distorted wave calculations to extend the scope of the studies of Levin and Eisenberg.<sup>16</sup> Since our primary interest lies in the examination of distortion effects arising from the residual core, the calculations utilize the factorized DWIA. The dominant effects of distortion will still be evident in spite of some breakdown in the factorization approximation.

The present calculations extend the energy range (to 300 MeV) and the mass range (to  $^{40}\text{Ca}$ ) of the previous DWIA calculations. These calculations are carried out in coordinate space allowing us to examine the degree of surface localization for specific conditions. Phenomenological pion optical

potentials which fit elastic scattering and therefore have the correct asymptotic behavior are used. Finally, calculations are carried out for the geometries examined in Ref. 15.

The DWIA formalism is discussed in detail in Sec. II. In Sec. III we present DWIA calculations of  $^{16}\text{O}, ^{40}\text{Ca}(\pi^+, \pi^+p)$  reactions for energies between 100 and 300 MeV. The calculations are carried out for a variety of geometries in order to examine the role of distortion effects both in studies emphasizing nuclear structure information and in studies attempting to explore the off-shell behavior of the projectile nucleon interaction. In Sec. IV we summarize the results.

## II. DWIA FORMULATION

We assume that the  $(\pi, \pi N)$  reaction proceeds via the quasifree knockout of a nucleon from the target nucleus. The distorted wave formalism for nucleon knockout has been developed by a number of authors. Briefly reviewing the DWIA following the discussion of Chant and Roos,<sup>17</sup> we introduce the impulse approximation to replace the transition operator by the two-body  $\pi + N$  operator. Furthermore, we assume that the corresponding  $t$  matrix varies sufficiently slowly that its arguments may be replaced by their asymptotic values. This approximation, coupled with a nonstatic approximation to decouple the wave equation for the exiting particles, leads us to the usual factorized DWIA expression for the  $A(\pi, \pi N)B$  three-body cross section. We consider a reaction  $A(\pi, \pi N)B$  in which the incoming pion knocks out a nucleon with angular momentum  $(l, j)$  from a target  $A$  with ground state spin  $J_i^\pi$  leading to a particular state in the final nucleus  $B$  with spin  $J_f^\pi$ . The incoming pion, emitted pion, and emitted nucleon have momenta and energies  $(\vec{k}_0, E_0)$ ,  $(\vec{k}_\pi, E_\pi)$ , and  $(\vec{k}_p, E_p)$ , respectively. Under these conditions, neglecting spin-orbit terms in the emitted nucleon-core potential, the factorized DWIA cross section can be written as

$$\frac{d^3\sigma}{d\Omega_\pi d\Omega_N dE_\pi} = C^2 S_{lj} |\langle \bar{t} \rangle|^2 \left\{ \frac{E_0 E_\pi E_N}{(2\pi)^5 (\hbar c)^6} \frac{k_\pi k_N C}{k_0} \right. \\ \left. \times \frac{1}{1 + \left[ \frac{E_N}{E_B} \right] \left[ 1 - \frac{k_0}{k_N} \cos\theta_N + \frac{k_\pi}{k_N} \cos(\theta_\pi + \theta_N) \right]} \right\} \sum_\lambda |T_{BA}^{al\lambda}|^2. \quad (5)$$

For simplicity in the following discussion, we rewrite Eq. (5) as

$$\frac{d^3\sigma}{d\Omega_\pi d\Omega_N dE_\pi} = \frac{2\pi}{\hbar v_\pi} \omega_B C^2 S_{lj} |\langle \bar{t} \rangle|^2 \\ \times \sum_\Lambda |T_{BA}^{al\Lambda}|^2, \quad (1)$$

where  $v_\pi$  is the relative velocity of the incoming pion and the target nucleus,  $\omega_B$  is the energy density of final states,  $C^2$  is an isospin Clebsch-Gordan coefficient, and  $S_{lj}$  is the single nucleon spectroscopic factor arising from the overlap of the initial and final nuclear states. The quantity  $|\langle \bar{t} \rangle|^2$  represents the half-off-the-energy shell  $\pi$ - $N$   $t$  matrix appropriately summed and averaged over the initial and final nucleon spins. It is evaluated for the asymptotic momenta. The quantity  $T_{BA}^{al\Lambda}$  is a distorted wave matrix element given by

$$T_{BA}^{al\Lambda} = \frac{1}{(2l+1)^{1/2}} \int \chi_B^{(-)*}(\vec{k}_B, \vec{r}) \chi_{NB}^{(-)*}(\vec{k}_{NB}, \vec{r}) \\ \times \chi_{\pi A}^{(+)}(\vec{k}_{\pi A}, \gamma \vec{r}) \phi_{l\lambda}^\alpha(\vec{r}) d^3r, \quad (2)$$

where the  $\chi$ 's represent distorted waves for the incoming pion, outgoing pion, and outgoing nucleon, and  $\gamma = B/(B+1)$ . The pion distorted waves are calculated with a modified Klein-Gordon equation containing a Kisslinger-type potential<sup>18</sup>, i.e.,

$$(-\nabla^2 + \mu^2)\chi_\pi = [E_\pi^2 - E_\pi V_c - U]\chi_\pi, \quad (3)$$

where

$$U\chi_\pi = -Ab_0\rho_0^2\rho\chi_\pi + Ab_1\nabla\cdot(\rho\nabla\chi_\pi). \quad (4)$$

The nucleon distorted wave is calculated using an optical model potential in a Schrödinger equation modified for relativistic effects.<sup>19</sup> The wave function  $\phi_{l\lambda}^\alpha$  is the bound single nucleon wave function arising from the overlap of the target and residual nucleus. In the spectator model limit in which the effect of the core  $B$  is negligible the distorted waves become plane waves and  $T_{BA}^{al\lambda}$  is proportional to the Fourier transform of this wave function.

Writing the expression for the cross section in detail, including the density of states, we have

$$\frac{d_3\sigma}{d\Omega_\pi d\Omega_N dE_\pi} = K \cdot C^2 S_{ij} \frac{d\sigma}{d\Omega} \Big|_{\pi+N} \sum_{\lambda} |T_{BA}^{al\lambda}|^2, \quad (6)$$

where  $K$  includes additional kinematic factors necessary to convert  $|\langle \bar{t} \rangle|^2$  to

$$\frac{d\sigma}{d\Omega} \Big|_{\pi+N},$$

the two-body  $\pi$ - $N$  half-shell cross section. Owing to the details of the spin summations,<sup>20</sup> for  $l > 0$  this cross section must be evaluated for scattering from a nucleon with polarization

$$P = \pm \frac{2}{2j+1} \frac{\sum_{m=-l+1/2}^{l-1/2} [(l + \frac{1}{2})^2 - m^2]^{1/2} \mathcal{J}_m (T_{BA}^{al,m+(1/2)} T_{BA}^{*al,m-(1/2)})}{\sum_{\lambda} |T_{BA}^{al\lambda}|^2}. \quad (7)$$

### III. DWIA CALCULATIONS

The DWIA calculations were carried out with a combination of the pion optical model code DUMIT<sup>21</sup> and the three-body DWIA code THREEDEE. In order to perform a systematic study of the distortion effects in the  $(\pi, \pi p)$  reaction over a range of energies, angles, and target nuclei, we would like to use "systematic" optical model potentials in which the dependence on energy and target mass has been clearly identified. Unfortunately, for pions there is little published on systematic analyses of pion elastic scattering. We have therefore followed our previous work on the  $(\pi, 2p)$  reaction,<sup>22</sup> and have used phenomenological choices of the  $s$ - and  $p$ -wave parameters  $b_0$  and  $b_1$ . For pion kinetic energies in excess of 100 MeV we have used the parametrization of Cottingham and Holtkamp<sup>23</sup> who obtain reasonable fits to  $\pi^\pm$  elastic scattering using free  $\pi$ -nucleon parameters from an energy approximately 30 MeV lower than the bombarding energy. For energies less than 100 MeV we have combined the results of Dytman *et al.*<sup>24</sup> and Amann *et al.*<sup>25</sup> The former publication shows that at 50 MeV an average set of fitted  $b_0$  and  $b_1$  provides reasonable fits to elastic scattering data from <sup>12</sup>C to <sup>54</sup>Fe. Amann *et al.*<sup>25</sup> show that a linear energy dependence of the  $b$ 's fits <sup>12</sup>C elastic scattering data from 28 to 88 MeV. We have therefore taken this parametrization and assumed it to be adequate for all  $N \approx Z$  nuclei. In our previous study of  $(\pi, 2p)$  distortion effects we found that the two sets of potentials do not extrapolate to each other and that at energies near 100 MeV the two gave results differing by as much as 30%. To avoid discontinuities in the cross section distributions for the present  $(\pi, \pi N)$  calculations, we have consistently used only one set of potentials and limited the calculations to either  $T_\pi > 100$  MeV or  $T_\pi < 100$  MeV.

For the emitted nucleon we have used the results of Nadasen *et al.*<sup>26</sup> The global potential presented in that work was obtained from a systematic analysis of proton elastic scattering data from Si to Pb with an energy range of 40 to 180 MeV. We believe this potential to be adequate even for <sup>16</sup>O to allow us to study the relative importance of distortion effects.

The bound single nucleon wave function  $\phi_{l\lambda}(\vec{r})$  was taken to be the solution of the Schrödinger equation for a nucleon bound in a Woods-Saxon potential. The geometrical parameters and spin-orbit strength of the potential were taken from the work of Elton and Swift<sup>27</sup> who fit elastic electron scattering and single particle separation energies.

In the present paper we have calculated DWIA cross sections for the  $(\pi^+, \pi^+ p)$  reaction only. Calculations of  $(\pi^-, \pi^- p)$  should provide very similar results in terms of distortion effects for the two ( $N = Z$ ) nuclei studied, the primary difference lying in the magnitude of the two-body cross section which is a multiplicative factor in the DWIA.

Finally, although many of the results presented which show the importance of distortion effects are independent of the two-body  $\pi^+ + p$  cross section, in those cases where the three-body cross section is calculated an on-shell prescription is used for the half-off-the-energy shell cross section. In particular, we have generally used the on-shell cross section at the rest energy of the  $\pi^+$  and proton in the final state (final energy prescription). The differences between this choice and an alternative choice using the on-shell cross section at an energy corresponding to the initial  $\pi^+ - p$  relative momentum (initial energy prescription used in Ref. 15) are also presented in some cases. The two-body  $\pi^+ + p$  cross sections were calculated using the phase shift analysis of Rowe, Salomon, and Landau.<sup>28</sup>

In the following subsections we present a variety

of results for the  $^{16}\text{O}(\pi^+, \pi^+p)^{15}\text{N}$  reaction to the ground state and 6.32 MeV level which involve the knockout of  $1p_{1/2}$  and  $1p_{3/2}$  protons, respectively, and for the  $^{40}\text{Ca}(\pi^+, \pi^+p)^{39}\text{K}$  reaction to the ground state and 2.53 MeV level in which  $1d_{3/2}$  and  $2s_{1/2}$  protons, respectively, are ejected.

### A. Energy sharing distributions—energy dependence

A common experimental geometry utilized for nuclear structure studies in  $(p, 2p)$  knockout reactions yields an energy sharing distribution. The angles of the two emitted particles are fixed, generally allowing zero or near zero recoil momentum for the residual nucleus ground state, and the cross section to a particular state measured as a function of the energy of one of the outgoing particles. In the

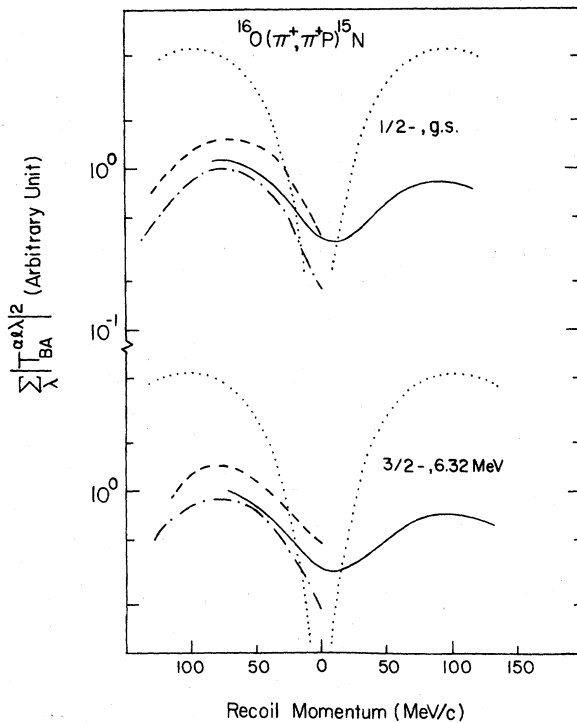


FIG. 1. Distorted momentum distributions for the  $^{16}\text{O}(\pi^+, \pi^+p)^{15}\text{N}$  reaction versus the recoil momentum of the residual nucleus corresponding to the knockout of  $1p_{1/2}$  (g.s.) and  $1p_{3/2}$  (6.32 MeV) protons. The calculations are for an energy sharing distribution with the emitted pion energy increasing to the right. The various curves represent results for different pion bombarding energies ( $\cdots$  PWIA;  $---$   $T_0=100$  MeV,  $\theta_\pi=115^\circ$ ,  $\theta_p=-24.81^\circ$ ;  $- \cdot - \cdot -$   $T_0=160$  MeV,  $\theta_\pi=115^\circ$ ,  $\theta_p=-24.29^\circ$ ;  $---$   $T_0=300$  MeV,  $\theta_\pi=115^\circ$ ,  $\theta_p=-22.46^\circ$ ).

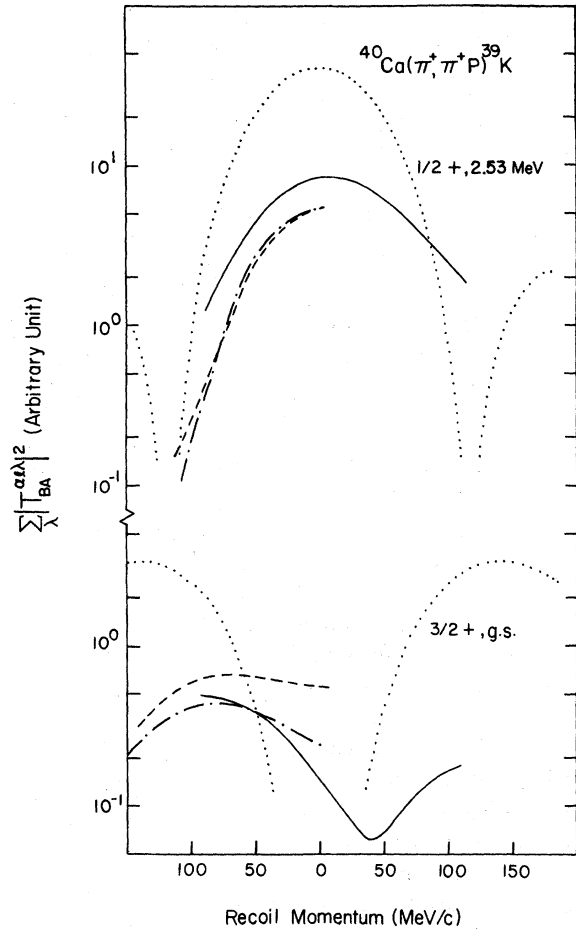


FIG. 2. Distorted momentum distributions for the  $^{40}\text{Ca}(\pi^+, \pi^+p)^{39}\text{K}$  reaction versus the recoil momentum of the residual nucleus corresponding to the knockout of  $1d_{3/2}$  (g.s.) and  $2s_{1/2}$  (2.53 MeV) protons. The calculations are for an energy sharing distribution with the emitted pion energy increasing to the right. The various curves represent results for different pion bombarding energies ( $\cdots$  PWIA;  $---$   $T_0=100$  MeV,  $\theta_\pi=115^\circ$ ,  $\theta_p=-25.38^\circ$ ;  $- \cdot - \cdot -$   $T_0=160$  MeV,  $\theta_\pi=115^\circ$ ,  $\theta_p=-24.66^\circ$ ;  $---$   $T_0=300$  MeV,  $\theta_\pi=115^\circ$ ,  $\theta_p=-22.67^\circ$ ).

plane wave limit the cross section is proportional to the square of the bound proton momentum space wave function, generally only weakly modulated by changes in the two-body cross section and kinematic factors. However, distortion effects can severely modify this distribution.

In Figs. 1 and 2 we present DWIA calculations for such a geometry for  $^{16}\text{O}$  and  $^{40}\text{Ca}(\pi^+, \pi^+p)$  at bombarding energies of 100, 160, and 300 MeV. The quantity plotted is the distorted momentum distribution

$$\sum_{\lambda} |T_{BA}^{al\lambda}|^2$$

which corresponds to data which have been divided by the two-body cross section and kinematic factors. Also shown is the corresponding plane wave calculation which, as noted earlier, is simply the bound proton momentum distribution. The distributions at 100 and 160 MeV are limited to one sign of the recoil momentum in order to avoid the transition through the region of  $T_{\pi}=100$  MeV requiring a discontinuous change in the pion potential. The pion angle was chosen to be  $\theta_{\pi}=115^{\circ}$ ; the proton angle being that necessary to allow zero recoil momentum for the ground state transition. This choice provides sufficient momentum transfer to the proton, and is similar to angle pairs presently being investigated experimentally.

For  $^{16}\text{O}$  the distortion effects do not destroy the  $p$ -wave character of the distribution. However, the minimum is both filled in and shifted to higher emitted pion energies, and the magnitude is reduced by about a factor of 5. The reduction near the maximum due to distortion is greatest for 160 MeV and least for 100 MeV, for which case the emitted pion is at low energy and therefore weakly interacting. The results for  $p_{3/2}$  and  $p_{1/2}$  are very similar. Note that the distortion effects narrow the distribution as a function of recoil momentum.

For  $^{40}\text{Ca}$  (Fig. 2) the distortion effects are generally more severe. For  $2s_{1/2}$  knockout, again the general shape is preserved, although in this case the distortion effects broaden the distribution. For this heavier nucleus, the 300 MeV cross section is reduced least and as expected the reduction due to distortion is greater than for  $^{16}\text{O}$ . The  $1d_{3/2}$  knockout calculations show results similar to those for  $^{16}\text{O}$  with the minimum shifted to higher  $T_{\pi}$  and filled in; at 100 MeV the minimum is almost nonexistent. Unlike the  $2s_{1/2}$  transition at the peak of the distribution (i.e., low energy emitted pions) the 100 MeV case is the least attenuated as found for  $^{16}\text{O}$ . Again the distorted momentum distributions are narrower than the plane wave results.

From Figs. 1 and 2 we see that the energy dependence of

$$\sum_{\lambda} |T_{BA}^{al\lambda}|^2$$

at the peak of the energy sharing distribution is not terribly strong, varying by roughly  $\pm 25\%$  over the energy range 100 to 300 MeV. Thus, if the DWIA predictions are correct, we expect the energy dependence of the cross section to be dominated by the product of the kinematic factor and the two-body

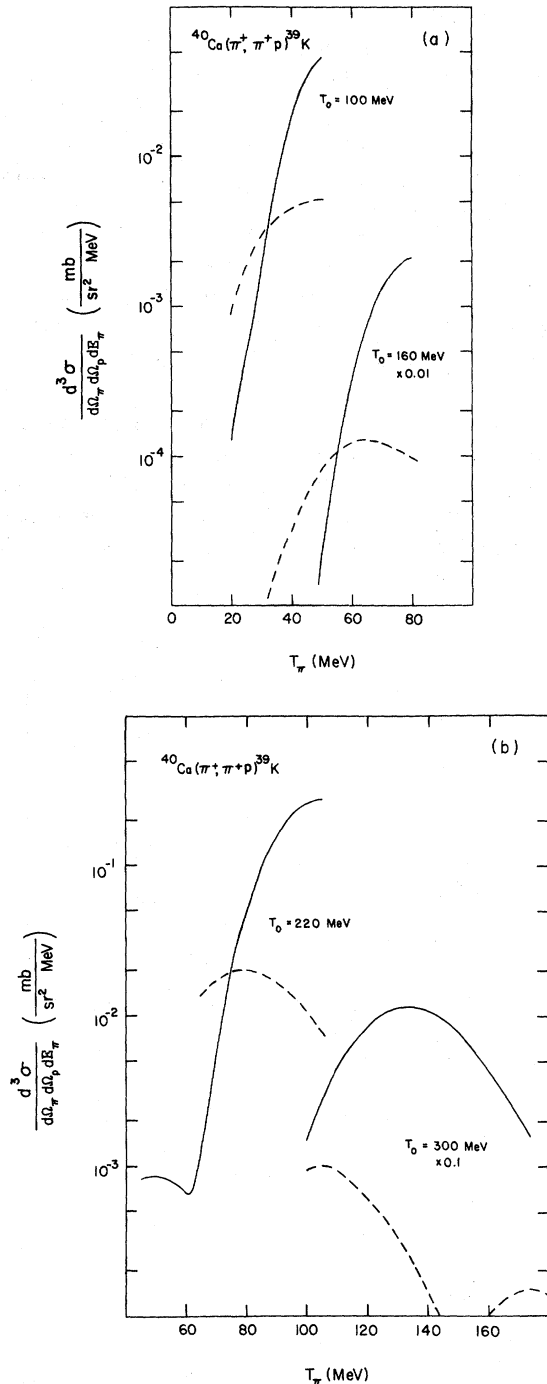


FIG. 3. (a) DWIA cross section for  $^{40}\text{Ca}(\pi^+, \pi^+ p)$  for  $2s_{1/2}$  (—) and  $1d_{3/2}$  (---) proton knockout with incident pions of 100 and 160 MeV. The calculations are for an energy sharing distribution with  $\theta_{\pi}=115^{\circ}$  and  $\theta_p$  chosen to allow zero recoil momentum for the ground state transition. The calculations assume a spectroscopic factor  $C^2S$  of unity, and employ the final energy prescription for  $(d\sigma/d\Omega)_{\pi^+ p}$ . (b) Same as (a) with incident energies of 220 and 300 MeV.

$\pi^+p$  cross section.

To provide an estimate of the absolute cross section and to show the effect of the kinematic and free cross section factors, we plot the energy sharing cross sections for the two  $^{40}\text{Ca}(\pi^+, \pi^+p)$  transitions in Fig. 3. For this graph we have assumed the final energy prescription for the two-body  $\pi^+p$  cross section, and a spectroscopic factor  $C^2S$  of unity, rather than the empirical occupation numbers. The cross section at the peak of the distribution increases with energy up to 220 MeV due to the increase in phase space and the two-body cross section. Above 220 MeV it falls, since the two-body cross section falls more rapidly than the phase space increases. These predicted cross sections are comparable to or larger than those measured in  $(p, 2p)$ . Unfortunately, currently available proton and pion beam intensities differ by several orders of magnitude in intensity.

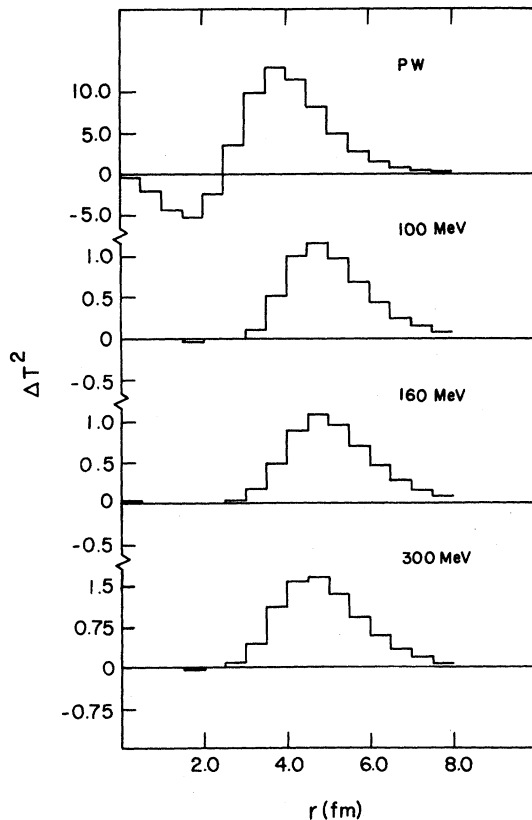


FIG. 4. Change in  $\sum_{\lambda} |T_{BA}^{al\lambda}|^2$  with radial cutoff for the  $^{40}\text{Ca}(\pi^+, \pi^+p)^{39}\text{K} (\frac{1}{2}^+, 2.5 \text{ MeV})$  reaction as a function of radius. The results are for the zero recoil momentum point at three bombarding energies. For comparison the plane wave calculation is also presented.

## B. Radial localization

To examine distortion effects in more detail it is useful to calculate the cross section as a function of a lower radial cutoff in the DWIA integrand. Previous DWIA calculations of knockout reactions have shown that this is a useful tool in understanding the radial regions of the nucleus contributing to a given reaction, and thereby the degree of surface localization. The most easily understood case for such a study is that of the knockout of an  $l=0$  nucleon for zero recoil momentum. Note that in the plane wave limit the integrand is simply  $[r^2\phi_l^\lambda(r)]$ , where  $\phi$  is the proton single particle wave function.

In Fig. 4 we present the results for  $^{40}\text{Ca}(\pi^+, \pi^+p)^{39}\text{K} (\frac{1}{2}^+, 2.53 \text{ MeV})$ . Plotted is the difference in

$$\sum_{\lambda} |T_{BA}^{al\lambda}|^2$$

for adjacent cutoff radii as a function of radius; i.e.,

$$\Delta(T^2) = \sum_{\lambda} |T_{BA}^{al\lambda}(r)|^2 - \sum_{\lambda} |T_{BA}^{al\lambda}(r + \Delta)|^2$$

where

$$\sum_{\lambda} |T_{BA}^{al\lambda}(x)|^2$$

is calculated with a lower radial cutoff of  $x$ . The comparison with plane waves clearly shows the strong absorption of the  $(\pi^+, \pi^+p)$  reaction in the nuclear interior at all three energies, with some slight increase in penetration and magnitude for 300 MeV. In general, the contribution to the cross section peaks near 5 fm with essentially no contribution arising from inside 3 fm.

It is interesting to consider this radial localization in the context of the effects due to Pauli blocking. The estimates by Jackson *et al.*<sup>15</sup> often show sizable differences (up to factors of 2 to 3 for specific geometries) in the two-body  $\pi^+p$  cross section calculated with no Pauli blocking ( $k_F=0$ ) and with full blocking ( $k_F=1.36 \text{ fm}^{-1}$ ). However, for the cases shown in Fig. 4 the primary yield arises from the region of 5 fm corresponding to approximately 7% of the  $^{40}\text{Ca}$  central density. This indicates that the blocking effects should be those corresponding to  $k_F < 0.7 \text{ fm}^{-1}$ . Therefore, based on the calculations of Ref. 15, one might expect Pauli blocking effects to be at most 20%, and generally less than 10%.

In order to place the  $(\pi^+, \pi^+p)$  reaction in perspective with other proton knockout reactions and their ability to sample the nucleus, we have per-

formed the same cutoff radius calculations for  $(e, ep)$ ,  $(p, 2p)$ , and  $(\alpha, \alpha p)$  reactions at energies for which experiments have been performed. These calculations, along with  $(\pi^+, \pi^+ p)$  at 160 MeV, are presented in Fig. 5. Note that the scale of the ordinate is significant since  $\Delta(T^2)$  is plotted, so that in the plane wave limit all reactions will give the same magnitude. It is clear from this plot that distortion effects in the  $(\pi^+, \pi^+ p)$  reaction are comparable to those found in the  $(p, 2p)$  reaction near 150 MeV. It is also clear that the  $(e, ep)$  reaction better samples the nuclear interior, the results being quite similar to the plane wave calculation. In contrast, the  $(\alpha, \alpha p)$  reaction is by far the most surface localized, sampling only the binding energy tail of the proton

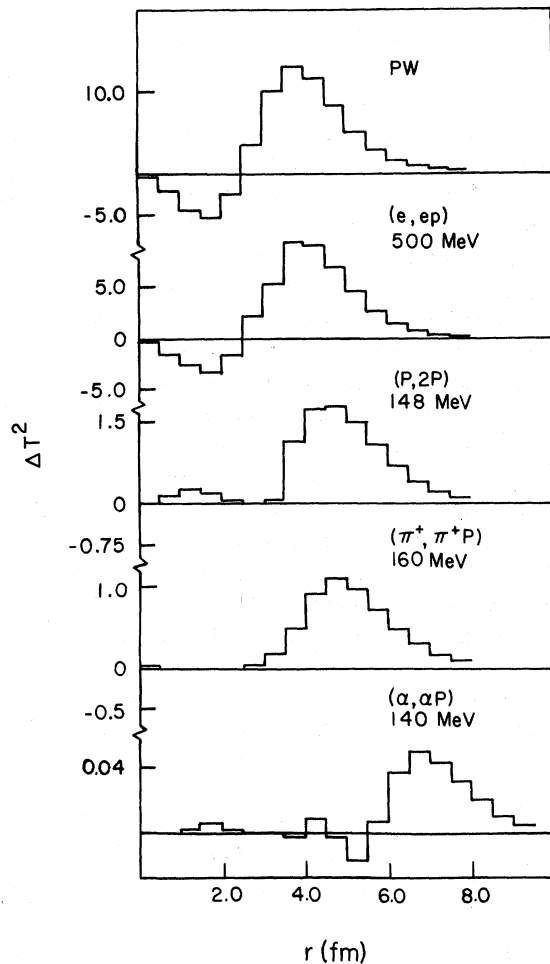


FIG. 5. Change in  $\sum_{\lambda} |T_{BA}^{a\lambda}|^2$  with radial cutoff as a function of radius. The calculations are for the knockout of a  $2s_{1/2}$  proton from  $^{40}\text{Ca}$  by various projectiles at the incident energies indicated in the figure. The calculations are for the zero recoil momentum point.

single particle wave function. Thus, since it is least modified by distortion effects, the  $(e, ep)$  reaction is by far the most satisfactory, with  $(\pi, \pi p)$  and  $(p, 2p)$  providing results comparable to each other.

### C. $\pi^+ - p$ cross sections and off-shell effects

Assuming the basic applicability of the quasifree knockout reaction mechanism, which has yet to be tested in detail experimentally, one can use the  $(\pi, \pi N)$  reaction in order to investigate the off-energy shell  $(\pi - N)$  interaction and/or effects due to the nuclear medium. With the flexibility of the three-body final state many experimental geometries are possible. However, as noted earlier, a thorough understanding of the distortion effects arising from interactions with the core is essential to the extraction of any detailed  $\pi - N$  interaction information.

To provide guidance for any future experimental studies of this type, we have carried out DWIA calculations for the rather standard experimental geometries used in studies of the dependence of the three-body cross section on the two-body light particle vertex; i.e., the  $\pi - N$  vertex in the present study. We not only show the effects of distortion, but also consider two on-shell approximations to the  $\pi - N$  interaction, which perhaps serve as an upper limit on the range of effects to be expected due to off-shell effects. In the following we investigate the dependence on bombarding energy, energy sharing, and angle.

One obvious study of the  $\pi - N$  vertex is a measurement of the dependence of the  $(\pi^+, \pi^+ p)$  cross section on bombarding energy, as had already been discussed in Sec. III A. We have shown that the energy dependence of the distortion effects is rather modest over the energy range 100 to 300 MeV. Thus, the  $(\pi^+, \pi^+ p)$  cross section to a large extent reflects the two-body  $\pi^+ + p$  cross section. A good candidate for such a study is the  $^{40}\text{Ca}(\pi^+, \pi^+ p)^{39}\text{K}(\frac{1}{2}^+, 2.53 \text{ MeV})$  transition for zero recoil momentum. At this point the cross section is large and not so sensitive to the treatment of distortion effects. A measurement in the energy range 100 to 300 MeV will indicate whether the  $\pi^+ + p$  resonance is shifted in energy and its width modified by the off-shell effects and/or nuclear medium effects.

A second study of the off-shell  $\pi - N$  cross section is that of the energy sharing distribution discussed in Sec. III A. Although the shape of the energy sharing distribution tends to be dominated by the single particle momentum distribution, modifications by the two-body  $\pi^+ + p$  cross section are sig-

nificant. To emphasize this two-body effect we have calculated the  $^{16}\text{O}(\pi^+, \pi^+p)^{15}\text{N} (\frac{3}{2}^-, 6.32 \text{ MeV})$  transition at 160 MeV. This transition has the most negative  $Q$  value of any considered here and therefore the most off shell. Furthermore, a bombarding energy near 160 MeV enhances the effect of the  $\pi^+p$  resonance, at least for the two prescriptions for the  $\pi^+p$  cross section considered here.

In Fig. 6 we present DWIA calculations for the energy sharing distribution for  $^{16}\text{O}(\pi^+, \pi^+p)^{15}\text{N} (\frac{3}{2}^-)$ . The upper panel shows the variation in the two-body  $\pi^+p$  cross section using the two on-shell prescriptions as a function of the emitted pion kinetic energy. Owing to the approximately  $-20 \text{ MeV}$   $Q$  value, the two prescriptions place the peak of the resonance at rather different outgoing pion energies. The effect on the energy sharing distribution is shown in the lower panel of Fig. 6. The choice of prescription strongly affects the ratio of the two peaks in the  $p$ -state distribution. The ratio of the left to right peak differs by 50% for our two choices of two-body cross sections. In this context it should be emphasized that Levin and Eisenberg<sup>16</sup> have shown that this peak ratio also depends on the applicability of the factorization approximation and

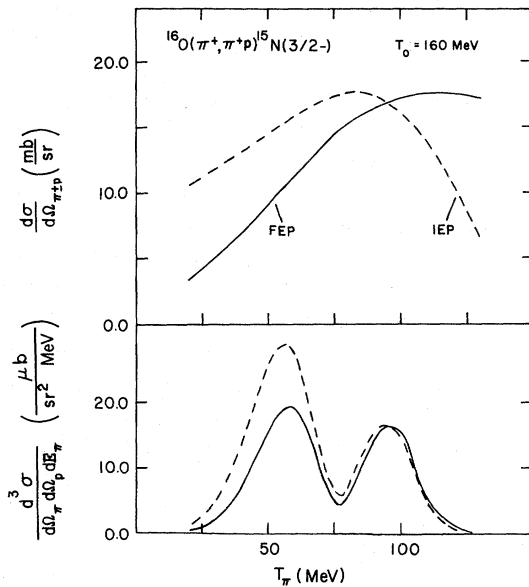


FIG. 6. DWIA energy sharing cross section for the  $^{16}\text{O}(\pi^+, \pi^+p)^{15}\text{N} (\frac{3}{2}^-, 6.2 \text{ MeV})$  reaction at 160 MeV. The top panel shows the two-body  $\pi^+p$  cross sections used in the calculations for two on-shell prescriptions. The lower panel shows the three-body cross section for the two prescriptions [— final energy prescription (FEP); - - initial energy prescription (IEP)] using a spectroscopic factor  $C^2S$  of unity.

the strength of the spin-orbit potential for the emerging proton. Thus, the use of such an energy sharing experiment to examine off-shell effects may require different angles, energies, and targets to specifically isolate any off-shell behavior. This measurement still has the advantage that important information can be extracted from a ratio measurement rather than relying on absolute cross section measurements.

A third experimental study of value in elucidating the role of the  $\pi$ - $N$  interaction in  $(\pi, \pi N)$  reactions is a study of the angular dependence of the  $(\pi, \pi N)$  reaction for a fixed value of recoil momentum. In the PWIA the momentum distribution is thereby fixed and the variation with angle reflects the variation with angle of the two-body cross section, aside from a known kinematic factor [see Eq. (6)]. Such a geometry has been used very effectively to examine the factorization approximation inherent in the DWIA for  $(p, 2p)$ ,<sup>29</sup>  $(p, p\alpha)$ ,<sup>30</sup> and  $(\alpha, 2\alpha)$  (Ref. 31) reactions.

For the  $(\pi, \pi N)$  reactions this experiment provides a combination of a test of the factorization approximation and a study of the angular dependence of the half-shell two-body cross section. Unfortunately, the two cannot be separated. However, with the strong angular and energy dependence of the  $\pi^+p$  cross section, careful measurements may provide suitable information on both aspects.

The value of such an experiment depends greatly on the importance of distortion effects and our ability to treat them properly. To estimate their importance we have carried out a calculation of the  $^{40}\text{Ca}(\pi^+, \pi^+p) (\frac{1}{2}^+, 2.53 \text{ MeV})$  transition with zero recoil momentum at an incident energy of 300 MeV. This bombarding energy was chosen to avoid the necessity of changing the pion optical model parameters at some point in the angular distribution.

The results of the DWIA calculations versus the pion laboratory scattering angle are presented in Fig. 7. The top panel shows the center-of-mass  $\pi^+p$  two-body scattering angle (both on-shell prescriptions give the same angle). The middle panel shows the ratio of the DWIA to PWIA cross section for each angle pair, and the bottom panel shows the quantity

$$K \cdot \sum_{\lambda} |T_{BA}^{\alpha\lambda}|^2$$

as defined in Eq. (6). These calculations show that unlike the cases studied in Refs. 24–26, the distortion effects are rather strongly angle dependent, varying by more than a factor of 4 from  $25^\circ$  to  $145^\circ$ . It is interesting to note that the distorted wave to

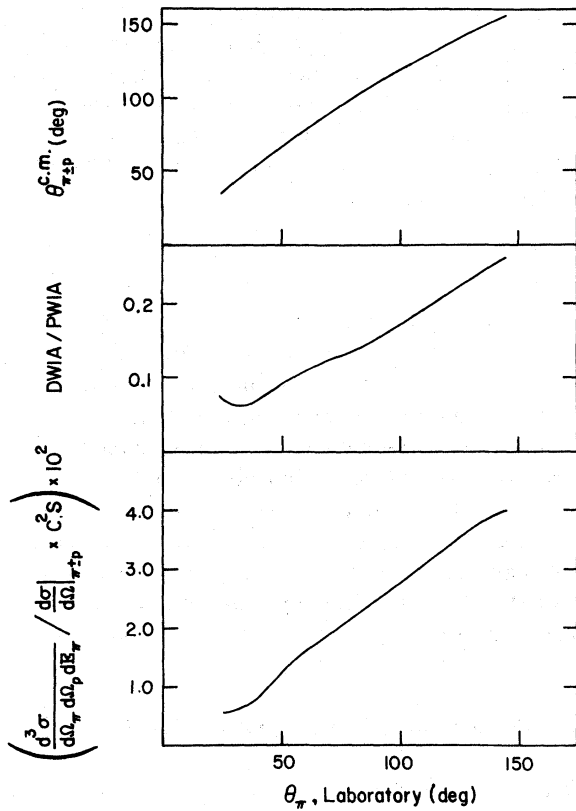


FIG. 7. Angular distribution for the  $^{40}\text{Ca}(\pi^+, \pi^+p)^{39}\text{K} (\frac{1}{2}^+, 2.5 \text{ MeV})$  reaction at 300 MeV. All calculations correspond to zero recoil momentum, the pion scattering angle being the abscissa and the proton angle chosen to allow  $p_3=0$ . The top panel shows the two-body  $\pi^+ + p$  scattering angle, the middle panel shows the ratio of distorted wave to plane wave calculations, and the bottom panel shows the quantity  $K \cdot \sum_{\lambda} |T_{BA}^{\alpha\lambda}|^2$  as defined in Eq. (6).

plane wave ratio is smallest for the small angles where the outgoing pion energy is greatest ( $\theta=25^\circ$ ,  $T_\pi=272.7 \text{ MeV}$ ), increasing as the angle is increased and the outgoing pion energy decreases to below the resonance ( $\theta=145^\circ$ ,  $T_\pi=113.0 \text{ MeV}$ ). This result suggests that the distortion effects due to the proton outweigh the greater absorption of the pion near resonance.

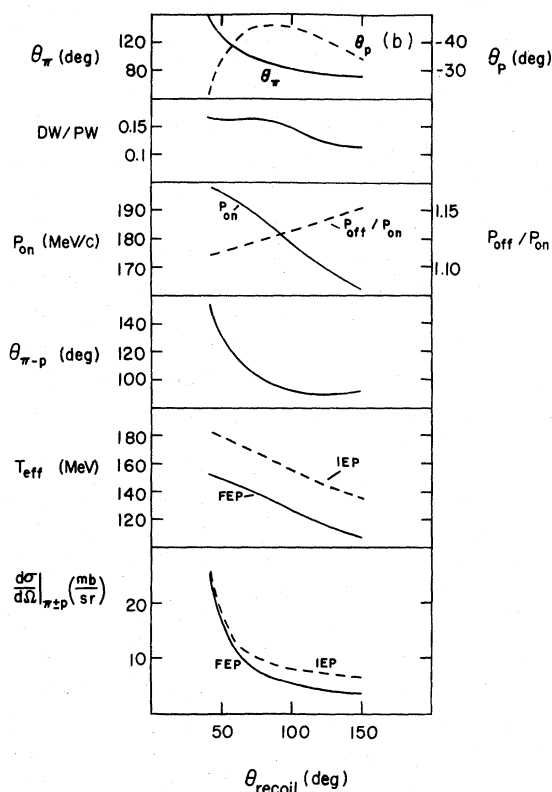
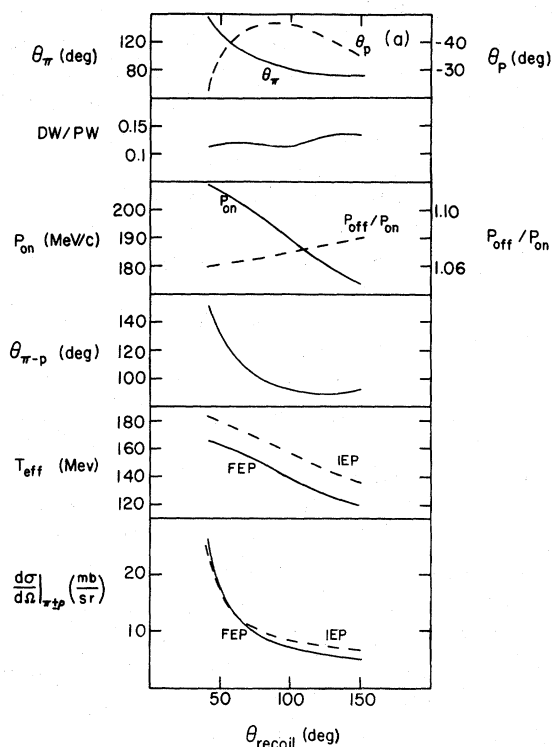
The calculations presented in Fig. 7 suggest that it may be very difficult to extract detailed information on the off-shell  $\pi^+ - p$  behavior from the angular distribution for fixed recoil momentum. Perhaps, at best, data of this type will provide support (or nonsupport) for the use of the factorized DWIA.

The final experimental geometry we wish to consider is the fixed condition geometry *A* proposed by

Ioannides and Jackson.<sup>32</sup> In particular, for a fixed bombarding energy the  $(\pi, \pi N)$  cross section is measured for various angle pairs such that the magnitude of the recoil momentum and the ratio of the kinetic energies of the outgoing detected particles  $\lambda = T_\pi / (T_\pi + T_p)$  are fixed. Thus, the various angle pairs correspond to changes in the direction of recoil of the residual nucleus. The calculations in Ref. 15 indicate a rather strong dependence of the cross section on the treatment of  $\pi - N$  interaction. However, no distorted wave calculations for this geometry have been carried out. Since for a given state in the residual nucleus the laboratory kinetic energies are constant, one might expect rather smaller changes in the distortion effects with change in angle pair.

Again, to examine the importance of distortion effects we have carried out a series of DWIA calculations for the  $^{16}\text{O}(\pi^+, \pi^+p)^{15}\text{N} (\frac{3}{2}^-, 6.32 \text{ MeV})$  and  $^{40}\text{Ca}(\pi^+, \pi^+p)^{39}\text{K} (\frac{3}{2}^-, 0.0 \text{ MeV})$  transitions at 160 MeV using the above geometry. The results are summarized in Fig. 8. The top panel of Fig. 8 shows the experimental pion and proton angle pairs required to achieve a particular recoil direction (abscissa) with a fixed recoil momentum of 100 MeV/c and  $\lambda \approx 0.5$ . The second panel confirms our expectation that distortion effects are reduced for this geometry. The ratio of distorted wave to plane wave calculation varies by only about 25% for  $^{40}\text{Ca}$  and by about 50% for  $^{16}\text{O}$ . This variation is greatly reduced compared to the results shown in Fig. 7 for the angular distribution. The third panel from the top shows the relative pion-proton momentum in the final state ( $p_{\text{on}}$ ) and the ratio of the relative momentum in the initial state ( $p_{\text{off}}$ ) to  $p_{\text{on}}$ . These are the same variables used by Redish, Stephenson, and Lerner<sup>33</sup> in their analysis of off-energy-shell effects in  $(p, 2p)$  reactions. The quantity  $p_{\text{on}}$  varies by about 20% over the range of recoil angles examined. The quantity  $p_{\text{off}}$  varies slightly less rapidly, the ratio  $p_{\text{off}}/p_{\text{on}}$  changing by a few percent. Obviously, the  $^{16}\text{O}$  case is further off shell.

The bottom three panels of Fig. 8 provide some indication of the expected off-energy effects by presenting two possible on-shell prescriptions for the half-shell cross section. For  $(p, 2p)$  reactions comparably off shell the proper half-shell cross section generally lies between these two extremes. We present the two-body  $\pi^+ - p$  c.m. scattering angle  $\theta_{\pi^+ - p}$  (common for the two prescriptions), the effective incident  $\pi^+$  laboratory energy for the two-body  $\pi^+ - p$  system ( $T_{\text{eff}}^{\pi^+ - p}$ ), and the calculated on-shell two-body cross section for  $T_{\text{eff}}^{\pi^+ - p}$  and  $\theta_{\pi^+ - p}$ . Notice for this geometry both the scattering angle and ef-



fective energy change, unlike the previous case in which only the scattering angle changes. For this particular bombarding energy and  $Q$  values the  $\pi^+p$  energies lie in the resonance region, thereby leading to different shapes for the two-body cross section obtained with the two prescriptions. The ratio of the cross sections

$$\frac{d\sigma}{d\Omega} \Big|_{\pi^+p}$$

for the two prescriptions varies with recoil angle ( $\theta_{\text{recoil}}=41^\circ \rightarrow 150^\circ$ ) by a factor of 1.4 for  $^{40}\text{Ca}$  and a factor of 1.74 for  $^{16}\text{O}$ . One would expect to be able to distinguish a difference as large as that predicted for  $^{16}\text{O}$ . Clearly the advantages of this geometry lie in the fact that the distortion effects are relatively constant, and thereby their variation is more likely to be predictable. Experiments carried out near 160 MeV may thus be able to improve our understanding of the off-shell effects by examining the dependence of the  $(\pi^+, \pi^+p)$  cross section on recoil angle.

#### IV. SUMMARY AND CONCLUSIONS

The present  $(\pi, \pi N)$  DWIA calculations for various targets, bombarding energies, and angles show large effects arising from the interaction of the incident and emitted particles with the residual nuclear core. Any theoretical treatment will necessarily have to include these effects. Furthermore, in the energy range studied, the distortion effects may be strongly energy dependent due to the presence of the  $\pi$ - $N$  resonance.

Two aspects of the  $(\pi, \pi N)$  reaction have been examined: the ability of the reaction to provide nuclear structure information or to provide information on the off-shell behavior of the  $\pi$ - $N$  interac-

FIG. 8. (a) Calculations for  $^{40}\text{Ca}(\pi^+, \pi^+p)^{39}\text{K}$  ( $\frac{3}{2}^+$ , 0.0 MeV) at 160 MeV using a geometry of Ref. 24 in which only the direction of recoiling nucleus varies (abscissa). The magnitude of recoil momentum is fixed at  $|p_3| = 100$  MeV/c and the ratio of the emitted pion to proton kinetic energies at  $\lambda=0.53$ . Displayed from top to bottom are the pion and proton scattering angles, the ratio of the distorted wave to plane wave calculation, the two-body momenta in the initial ( $p_{\text{off}}$ ) and final ( $p_{\text{on}}$ ) states, the two-body scattering angle, the effective two-body scattering energy, and the two-body cross section for two on-shell prescriptions. (b) Calculations for  $^{16}\text{O}(\pi^+, \pi^+p)^{15}\text{N}$  ( $\frac{3}{2}^-$ , 6.32 MeV) at 160 MeV with  $|p_3| = 100$  MeV/c and  $\lambda=0.52$  [see (a)].

tion. In the former case the calculations suggest that the shapes of energy sharing distributions will reflect the behavior of the single particle wave function. However, the strong distortion effects indicate that the extraction of any detailed nuclear structure information will depend on the specific treatment of the distorting potentials. Thus, we expect sensitivity to the choice of the pion optical model potentials, which are rather poorly understood at the present time. More importantly, calculations of the radial localization show that  $(e, ep)$  reactions are best for providing information on the single particle wave function, and that  $(p, 2p)$  and  $(\pi, \pi p)$  are comparable. Considering the greater experimental ease with which  $(p, 2p)$  experiments can be performed and the better knowledge of proton optical model potentials, it seems difficult to justify  $(\pi, \pi p)$  reactions for general nuclear structure studies. Rather we see studies such as measurements of the energy sharing distributions as providing tests of the treatment of the reaction mechanism. One would like such data at various energies for various targets to test models such as the DWIA presented here.

Studies of off-shell effects seem to us to be more

promising, at least if one can show the basic applicability of the DWIA, or other suitably simple models. The present calculations indicate that one of the best geometries for such experimental studies is that proposed by Ioannides and Jackson.<sup>27</sup> The primary advantage of this geometry is that the variation in distortion effects is relatively small, so that the extraction of the  $\pi$ - $N$  energy and angular dependence will probably not be as sensitive to the choice of the pion optical model potentials. Other studies such as the energy sharing distribution and the quasifree angular distribution will provide tests of the reaction model, as well as the off-shell behavior, provided that an improved knowledge of the distorting potentials is forthcoming.

#### ACKNOWLEDGMENTS

This work was supported in part by the National Science Foundation. The authors would like to thank the University of Maryland Computer Science Center for their generous allocation of computer time for carrying out the DWIA calculations.

- <sup>1</sup>E. Piasezky *et al.*, in *Proceedings of the Ninth International Conference on High Energy Physics and Nuclear Structure, Versailles, 1981*, edited by P. Catillon, P. Radvanyi, and M. Porneuf (North-Holland, Amsterdam, 1982).
- <sup>2</sup>E. Piasezky *et al.*, see Ref. 1, Abstract H32.
- <sup>3</sup>F. Goetz *et al.*, see Ref. 1, Abstract H33.
- <sup>4</sup>T. S. Bauer *et al.*, see Ref. 1, Abstract H34.
- <sup>5</sup>P. A. M. Gram *et al.*, see Ref. 1, Abstract H36.
- <sup>6</sup>H. J. Ziock *et al.*, *Phys. Rev. C* **22**, 907 (1980).
- <sup>7</sup>H. J. Ziock *et al.*, *Phys. Rev. Lett.* **43**, 1919 (1979).
- <sup>8</sup>R. J. Ellis *et al.*, *Phys. Lett.* **88B**, 253 (1979).
- <sup>9</sup>P. G. Roos, in *Momentum Wave Functions—1976 (Indiana University)*, Proceedings of the Workshop/Seminar on Momentum Wave Function Determination in Atomic, Molecular, and Nuclear Systems, AIP Conf. Proc. No. 36, edited by D. W. Devins (AIP, New York, 1977).
- <sup>10</sup>J. Mougey *et al.*, *Nucl. Phys.* **A262**, 461 (1976); A. Nadasen *et al.*, *Phys. Rev. C* **19**, 2099 (1979).
- <sup>11</sup>R. Bhowmik, Ph.D. thesis, University of Maryland, 1975 (unpublished).
- <sup>12</sup>Morton M. Sternheim and Richard R. Silbar, *Phys. Rev. C* **21**, 1974 (1980).
- <sup>13</sup>M. M. Sternheim and R. R. Silbar, *Phys. Rev. Lett.* **34**, 824 (1975).
- <sup>14</sup>P. Varghese, R. R. Silbar, and M. M. Sternheim, *Phys. Rev. C* **14**, 1893 (1976).
- <sup>15</sup>D. F. Jackson, A. A. Ioannides, and A. W. Thomas, *Nucl. Phys.* **A322**, 493 (1979).
- <sup>16</sup>E. Levin and J. M. Eisenberg, *Nucl. Phys.* **A355**, 277 (1981).
- <sup>17</sup>N. S. Chant and P. G. Roos, *Phys. Rev. C* **15**, 57 (1977).
- <sup>18</sup>E. H. Auerbach, D. M. Fleming, and M. M. Sternheim, *Phys. Rev.* **162**, 1683 (1967).
- <sup>19</sup>A. Nadasen *et al.*, *Phys. Rev. C* **23**, 1023 (1981).
- <sup>20</sup>G. Jacob *et al.*, *Nucl. Phys.* **A257**, 517 (1976).
- <sup>21</sup>E. Rost, private communication.
- <sup>22</sup>P. G. Roos, L. Rees, and N. S. Chant, *Phys. Rev. C* **24**, 2647 (1981).
- <sup>23</sup>W. B. Cottingham and D. B. Holtkamp, *Phys. Rev. Lett.* **45**, 1828 (1980).
- <sup>24</sup>S. A. Dytman *et al.*, *Phys. Rev. C* **19**, 971 (1979).
- <sup>25</sup>J. F. Amann *et al.*, *Phys. Rev. C* **23**, 1635 (1981).
- <sup>26</sup>A. Nadasen *et al.*, *Phys. Rev. C* **23**, 1023 (1981).
- <sup>27</sup>L. R. B. Elton and A. Swift, *Nucl. Phys.* **A94**, 52 (1967).
- <sup>28</sup>Glenn Rowe, Martin Salomon, and Rubin H. Landau, *Phys. Rev. C* **18**, 584 (1978).
- <sup>29</sup>P. G. Roos *et al.*, *Phys. Rev. Lett.* **40**, 1429 (1978).
- <sup>30</sup>P. G. Roos *et al.*, *Phys. Rev. C* **15**, 69 (1977).
- <sup>31</sup>C. W. Wang *et al.*, *Phys. Rev. C* **21**, 1705 (1980).
- <sup>32</sup>A. A. Ioannides and D. F. Jackson, *Nucl. Phys.* **A308**, 305 (1978).
- <sup>33</sup>E. F. Redish, G. J. Stephenson, and G. M. Lerner, *Phys. Rev. C* **2**, 1665 (1970).